Fast light-particle production for the $^{11}B+^{12}C$ and $^{10}B+^{13}C$ reactions

J. F. Mateja and J. Garman
Department of Physics, Tennessee Technological University, Cookeville, Tennessee 38501

A. D. Frawley
Department of Physics, Florida State University, Tallahassee, Florida 32306
(Received 27 April 1983)

The fast light-particle yield for the $^{10}B+^{13}C$ and $^{11}B+^{12}C$ reactions has been studied at a bombarding energy of 54 MeV. The outgoing particles, whose spectra peak at an energy which corresponds approximately to the beam velocity, are attributed to projectile breakup. The predictions of a Serber-type projectile breakup model with no free parameters other than an overall normalization were compared with the shapes of the energy spectra and the angular distributions of all outgoing particles except for protons and alpha particles. For these exit channels, the breakup cross section is masked by a strong evaporation component. For those exit channels where a comparison could be made, the breakup model described the experimental data reasonably well. The magnitudes of the total breakup cross sections for the $^{10}B+^{13}C$ and $^{11}B+^{12}C$ systems are 290 mb and 193 mb, respectively.

[NUCLEAR REACTIONS $^{12}C(^{11}B,X)$ and $^{13}C(^{10}B,X)$, $X=$p,d,t,α,^{6}Li, ^{7}Li,^{7}Be,^{9}Be, $E=54$ MeV, $\theta=7.5°$ to 45°; measured $d^2\sigma/d\Omega\, dE$.]

I. INTRODUCTION

The distribution of the total strength is an important question in the study of the macroscopic properties of heavy-ion reactions. We have studied[1,2] the fusion and total reaction cross sections for the four entrance channels which lead to the ^{23}Na compound nucleus and have found, as is the case in other fusion studies in this mass and energy region,[3,4] that the total fusion cross section is considerably smaller than the total reaction cross section. The present investigation, a study of the fast light-particle yield, was undertaken in an attempt to locate this missing cross section.

It is known that deuterons and alpha particles break up readily in the field of the target nucleus.[5,6] More recently, the importance of this process has become apparent for heavier projectiles.[7–10] In this light we have looked at reaction products lighter than the beam for the $^{11}B+^{12}C$ and $^{10}B+^{13}C$ systems. While it is now generally believed that the breakup process is strong at high incident energies, the present work was undertaken at a relatively low beam energy of 54 MeV. Whatever the process is that is responsible for the missing total reaction strength, our present fusion and total reaction cross section data suggest that it begins at energies near the Coulomb barrier for these two systems.

II. EXPERIMENTAL PROCEDURE

Beams of ^{10}B and ^{11}B with laboratory energies of 54 MeV were obtained from the Florida State tandem Van de Graaff accelerator. Self-supporting ^{12}C and ^{13}C targets were used in a carbon-free, cryogenically pumped scattering chamber. No evidence was seen in the elastic scattering data of an appreciable oxygen contaminant. The reaction products were mass and Z identified with conventional E-ΔE telescopes. The energy spectra of the various outgoing particles were measured over an angular range from 7.5° to 45° in the laboratory. The energy calibration of the spectra was obtained by elastically scattering deuterons and ^{7}Li from a thin gold target over a wide range of beam energies.

III. RESULTS AND ANALYSIS

The energy spectra for all light particles produced in the $^{11}B+^{12}C$ reaction at an angle of 17.5° are presented in Figs. 1–3. The energy spectra for the $^{10}B+^{13}C$ reaction are shown in Figs. 4–6. While some discrete lines can be seen in several of the spectra, each spectrum is dominated, for the most part, by a broad continuum peak. It can clearly be seen that the energy centroids for these continuum peaks shift to lower energies as the mass of the detected particle decreases. This feature of the energy spectra is predicted by the simplest of breakup models. In such calculations, it is assumed that the detected particle is merely a spectator whose velocity is unaltered during the interaction. A particle of mass m would therefore be emitted in the $^{11}B+^{12}C$ reaction with an energy $m/11$ times the energy of the elastically scattered particles and with an energy of $m/10$ for the $^{10}B+^{13}C$ reaction. These energies, indicated by arrows in Figs. 1–6, match the continuum peak centroids reasonably well.

A more realistic model has also been used to describe

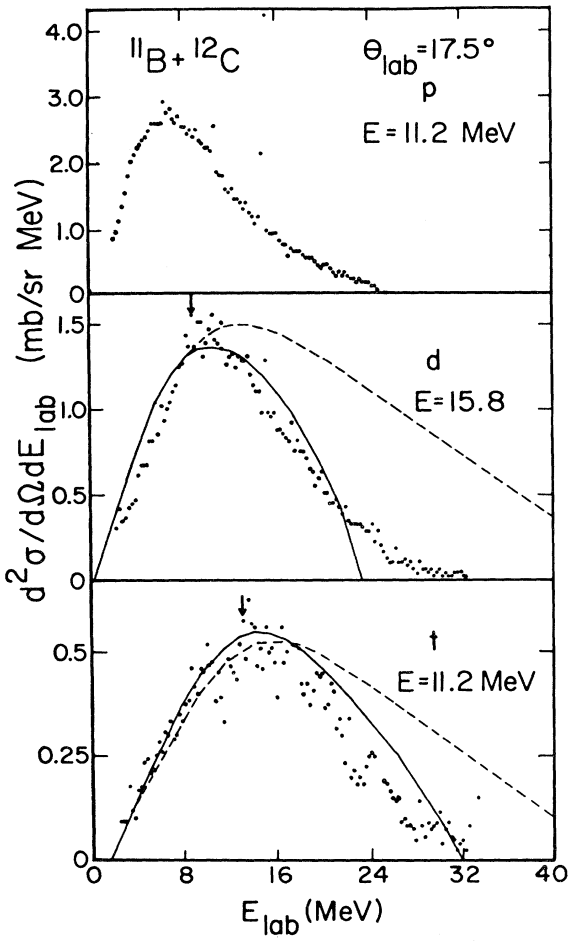

FIG. 1. The energy spectra of p, d, and t produced in the $^{11}B+^{12}C$ reaction at $E_{lab}=54$ MeV and $\theta_{lab}=17.5°$. The dashed and solid curves represent fragmentation model predictions of the energy distribution of the outgoing particle assuming either a two- or three-body final state. The energy listed along with each fragment is the energy required to separate the projectile into that fragment pair.

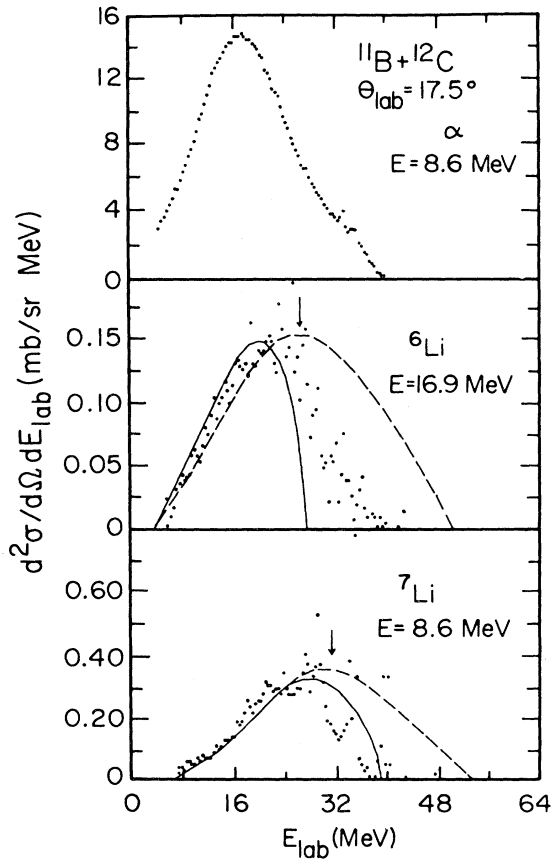

FIG. 2. The energy spectra of α, ^{6}Li, and ^{7}Li particles produced in the $^{11}B+^{12}C$ reaction at $E_{lab}=54$ MeV and $\theta_{lab}=17.5°$. For an explanation of the curves, see Fig. 1 and the text.

the breakup process. In this model,[5,11] the final momentum of the detected fragment is determined by both the velocity of the projectile and the intrinsic momentum of the fragment relative to the remainder of the projectile mass. The differential cross section for this process can be written as

$$d^2\sigma/d\Omega\, dE = KT^2\varphi\ , \tag{1}$$

where K is a normalization constant, T is the transition matrix element which accounts for the intrinsic momentum of the fragment, and φ is the phase space factor which takes into account the energy and momentum brought into the system by the projectile. The transition matrix is proportional to the internal momentum distribution of the fragment in the projectile,

$$|T|^2 \propto \left|\psi\left[P_1-\frac{m_1}{m_B}P_B\right]\right|^2\ , \tag{2}$$

where the subscripts 1 and B refer to the detected particle and the beam, respectively, and $\psi(P)$ is the projectile wave function in momentum space. A Yukawa potential of the form

$$\psi(r)=a^{1/2}(e^{-\alpha r})/r \tag{3}$$

was used to describe the relative wave function of the fragment inside the projectile coordinate space, where α is chosen to give the correct separation energy, i.e., $\alpha=(2\mu E_s)^{1/2}/\hbar$.

The form of the phase space factor depends on the reaction process involved. Two reaction mechanisms were considered. In the first, it was assumed that after the breakup of the projectile one of the fragments is captured by the target nucleus. As can be seen in Fig. 7(a), this results in a two-body final state. Such a process is more commonly called direct transfer to the continuum. The other reaction process assumed that neither fragment is captured after the breakup of the projectile. This process

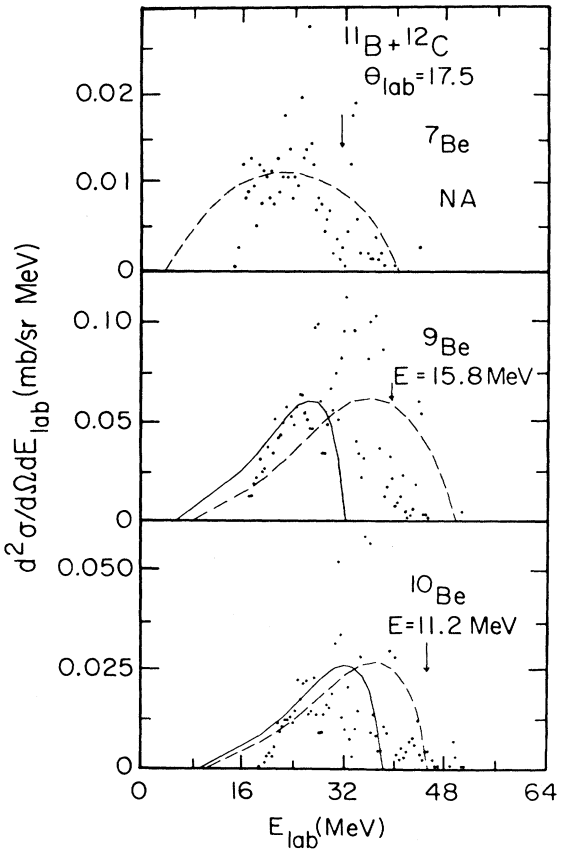

FIG. 3. The energy distribution of ^{7}Be, ^{9}Be, and ^{10}Be particles produced in the $^{11}B+^{12}C$ reaction at $E_{lab}=54$ MeV and $\theta_{lab}=17.5°$. For an explanation of the curves, see Fig. 1 and the text.

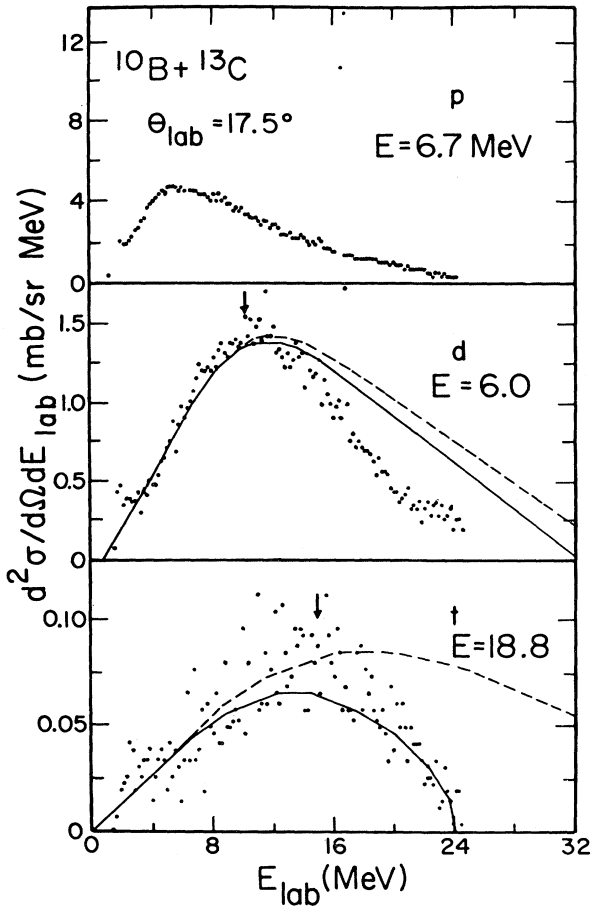

FIG. 4. The energy distribution of p, d, and t produced in the $^{10}B+^{13}C$ reaction at $E_{lab}=54$ MeV and $\theta_{lab}=17.5°$. For an explanation of the curves, see Fig. 1 and the text.

leaves three bodies in the final state as illustrated in Fig. 7(b).[12]

While the transition matrix elements for both of the above processes are the same, the phase space factors are not. The phase space factor for the three-body final state is

$$m_1P_1\int dP_2dP_T\delta(P_1+P_2+P_T-P_B)\times\delta(E_1+E_2+E_T+E_S-E_B)\,, \quad (4)$$

where the subscript 2 refers to the unobserved fragment and T refers to the target nucleus. The phase space factor for the two-body final state is

$$m_1P_1m_2P_2\,. \quad (5)$$

The major difference between these two cases is the difference in the Q values for the two reaction processes.

The above formulas are for plane incoming and outgoing waves. The simplest correction for Coulomb distortion of these waves is the local momentum approximation, a technique frequently used in electron scattering. We have, therefore, replaced the asymptotic momenta in Eq. (2) with their effective local values at the point of interaction,

$$P_{\text{eff}}=2m\,(E-E_C)^{1/2}\,, \quad (6)$$

where the Coulomb energy, E_C, was calculated at the touching distance, i.e., $1.2(A_B^{1/3}+A_T^{1/3})$. While the touching distance was used, the results of the calculation were not very sensitive to the exact separation.

The results of the calculations for the various outgoing light particles for both two- and three-body processes are presented in Figs. 1—6 as dashed and solid lines, respectively. Also shown in these figures is the energy required to dissociate the projectile into each fragment pair. Before comparing the various exit channels with the calculations it should be mentioned that we do not expect to be able to obtain either the proton or alpha particle breakup cross sections. For these exit channels it is well known that a strong compound nucleus evaporation component exists. At present there is no reliable means by which we can separate the proton or alpha particle events arising from breakup from those due to compound nucleus evaporation. We have not, therefore, presented the breakup calcu-

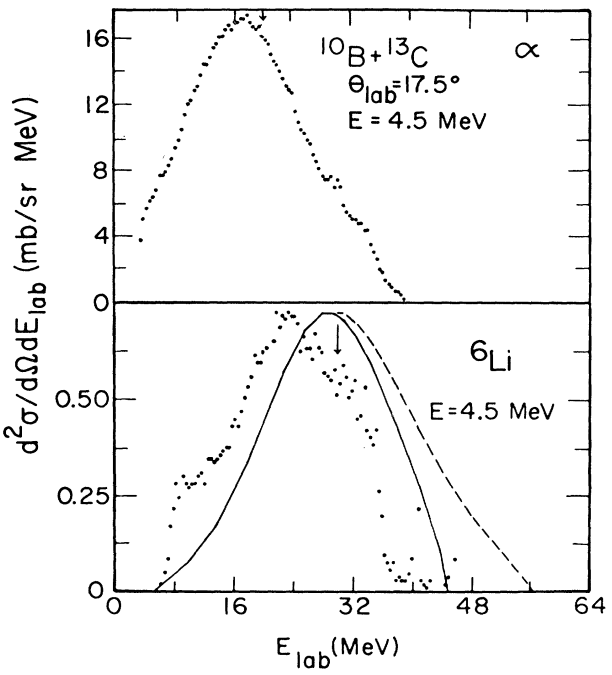

FIG. 5. The energy distribution of α and ^{6}Li particles produced in the $^{10}B+^{13}C$ reaction at $E_{lab}=54$ MeV and $\theta_{lab}=17.5°$. For an explanation of the curves, see Fig. 1 and the text.

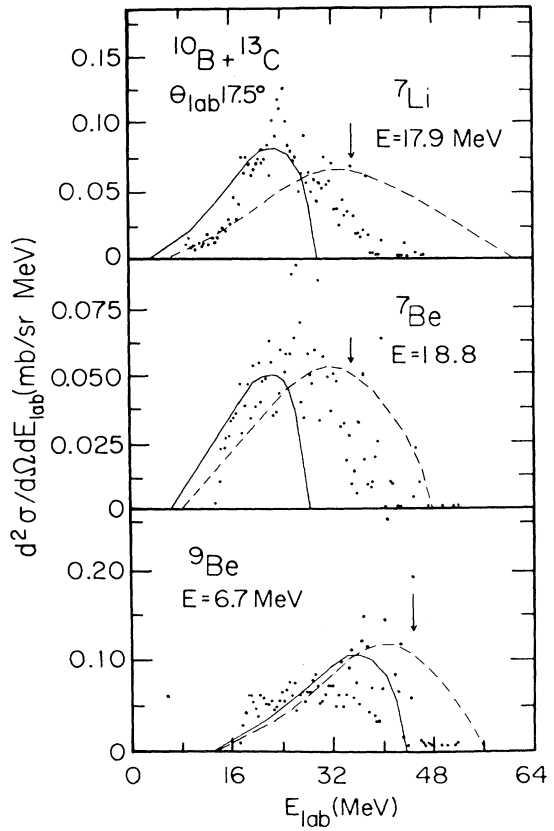

FIG. 6. The energy distribution of ^{7}Li, ^{7}Be, and ^{9}Be particles produced in the $^{10}B+^{13}C$ reaction at $E_{lab}=54$ MeV and $\theta_{lab}=17.5°$. For an explanation of the curves, see Fig. 1 and the text.

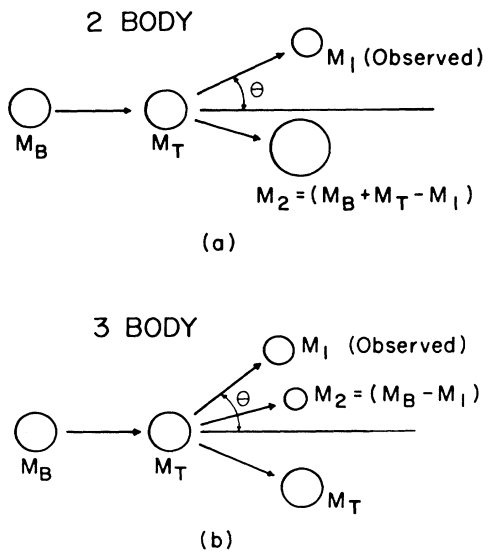

FIG. 7. (a) Schematic representation of projectile breakup followed by capture of one of the fragments. (b) a schematic representation of breakup with both breakup particles remaining free. The reactions represented in (a) and (b) result in two- and three-body final states, respectively.

lations for these exit channels.

For the $^{11}B+^{12}C$ breakup data, we see in Figs. 1 and 3 that the d, t, and ^{7}Li spectra are all well described by the calculation which assumed a reaction mechanism leading to a three-body final state. This, of course, does not rule out a two-body component in any of these exit channels. As a matter of fact, there must be a two-body component in the ^{7}Li data since several discrete states in ^{16}O can readily be identified. For the ^{7}Be exit channel, the three-body final state is energetically forbidden. For ^{7}Be, shown in Fig. 3, we find that the two-body calculation describes the behavior of these data very well. The remaining three spectra, ^{6}Li, ^{9}Be, and ^{10}Be are not particularly well described by either calculation. It would seem, however, that some combination of the two reaction processes could account for the experimental data.

The spectra of outgoing particles for the $^{10}B+^{13}C$ entrance channel, displayed in Figs. 4—6, are also reasonably well described by the calculations. The three-body reaction mechanism provides an adequate description of the d, t, ^{6}Li, and ^{9}Be spectra. Again, however, the presence of discrete peaks provides evidence of a two-body component in these energy spectra (in particular, see the ^{9}Be data). The ^{7}Li and ^{7}Be spectra are not particularly well described by either reaction mechanism. Again it would seem that some combination of the two reaction processes could account for the experimental data.

The calculations can also be used to describe the experimental angular distributions as shown in Figs. 8 and 9. The calculated angular distributions have been normalized to the data at 22.5°. We find that the general trend of the experimental angular distributions is reasonably well

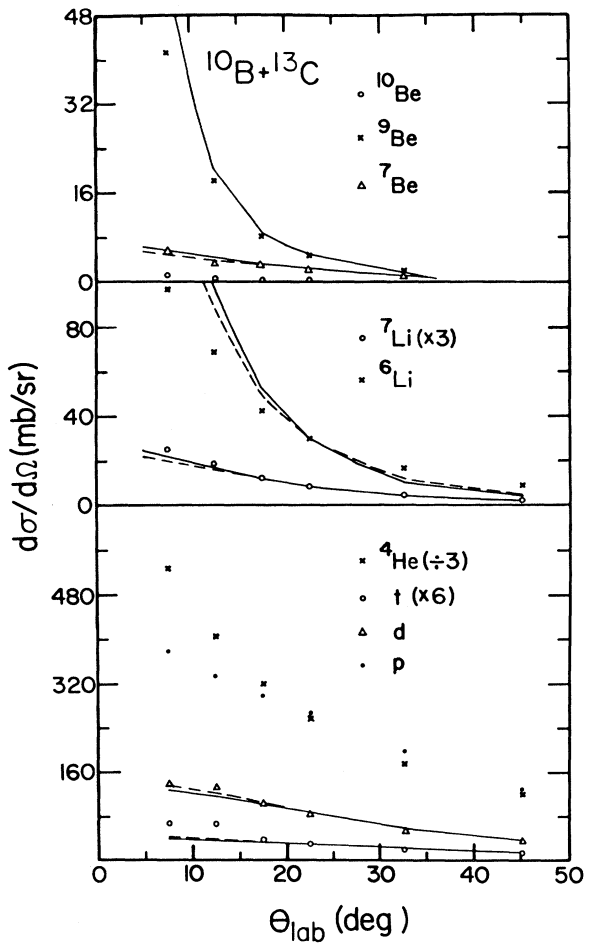

FIG. 8. Angular distributions of particles emitted in the $^{10}B+^{13}C$ reaction at $E_{lab}=54$ MeV. The dashed and solid curves represent fragmentation model predictions of the angular distributions of the outgoing particles assuming either a two- or three-body final state, respectively. The calculated angular distributions have been normalized to the data at 22.5°. For the ^{9}Be data, the calculated two- and three-body curves fall on the same line.

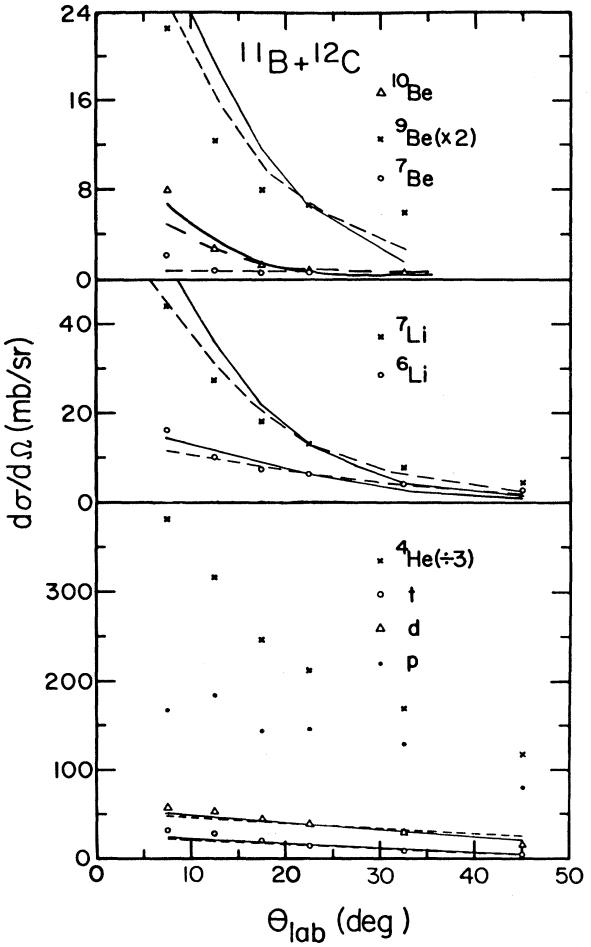

FIG. 9. Angular distributions of particles emitted in the $^{11}B+^{12}C$ reaction at $E_{lab}=54$ MeV. The dashed and solid curves represent fragmentation model predictions of the outgoing particles assuming either a two- or three-body final state, respectively. The calculated angular distributions have been normalized to the data at 22.5°.

reproduced by the calculations. Unfortunately, due to the close similarity of the calculated two- and three-body angular distributions, it is impossible to say which is favored by the experimental data.

One feature which becomes apparent after studying the data for both entrance channels is that those exit channels which require the smallest breakup energy (i.e., require the least amount of energy to dissociate the projectile into two fragments) are, in general, the ones best described by the three-body calculations, and also the channels which have the largest breakup cross sections. The angle integrated cross sections for the various exit channels are presented in Figs. 10 and 11. Again we must keep in mind that the proton and alpha particle groups are expected to contain a substantial evaporation component. The energy required to dissociate the projectile into a particular fragment pair is listed at the top of each column. As can be seen in Fig. 10, the d and ^{6}Li data for the $^{10}B+^{13}C$ entrance channel have (apart from p and α) the smallest breakup energies and the largest integrated cross sections. The same general features are also apparent in the $^{11}B+^{12}C$ data displayed in Fig. 11. That the exit channels with the smallest breakup energies have the largest cross sections is even more apparent when the reaction products for the two entrance channels are compared in Fig. 12. For a particular exit channel, the system with the lower breakup energy has the larger cross section.

In determining the total breakup cross section for the two systems, all exit channels except for the proton and alpha particle were included. Two questions must be addressed since the deuteron and triton yields have been included in the total breakup cross section: (1) What frac-

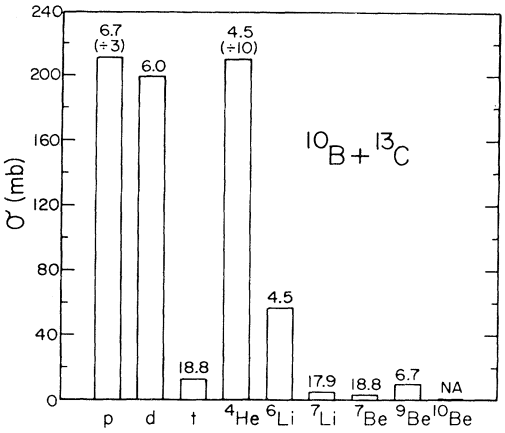

FIG. 10. Angle-integrated cross sections for the outgoing light particles produced in the $^{10}B+^{13}C$ reaction at 54 MeV.

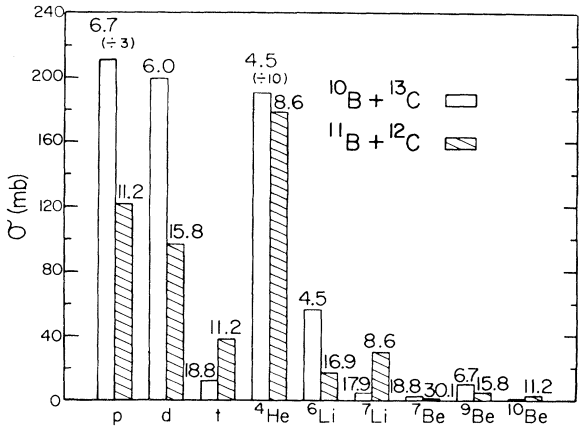

FIG. 12. A comparison of the relative distributions of the angle-integrated breakup cross sections for the $^{10}B+^{13}C$ and $^{11}B+^{12}C$ reactions. Both the ^{10}B and ^{11}B bombarding energies were 54 MeV.

tion of the deuteron and triton yields are due to compound nucleus evaporation? (2) Does this introduce a double counting problem: that is, are both fragments counted in a single breakup event?

The number of deuterons arising from compound nucleus evaporation may be estimated from a recent systematic study in this mass region by Xenoulis *et al.*[13] In this study the deuteron/pn evaporation cross-section ratio was investigated. To set an upper limit on the number of evaporation deuterons for the present entrance channels, we have assumed that all of the protons observed in the present experiment arise from pn evaporation. Since the protons we are observing can arise from other evaporation decay chains and breakup, such an assumption obviously overestimates the actual number of protons arising from pn evaporation. The upper limit on the deuteron cross section arising from compound nucleus evaporation is found to be less than 5 mb for both entrance channels. As can be seen in Figs. 10 and 11, this represents a very small fraction of the total deuteron strength. While we have no similar study involving tritons, we will assume a similar result.

When determining the total breakup cross section, care must be taken to ensure all breakup channels are included and that none of the exit channels are counted twice. Whether there is a double counting problem depends on whether the system is left in a two- or three-body final state. First, let us consider a reaction process leading to the three-body final state. The various breakup channels for the ^{10}B and ^{11}B projectiles are listed in column two of Table I. In evaluating the total breakup cross section, we have excluded the proton and alpha particle yields owing to our inability to distinguish between evaporation and breakup events. Since we only count the heavy particles in these channels, no double counting problem is encountered. The primary source of deuterons when a ^{10}B projectile breaks up is the d-^{8}Be exit channel. Since ^{8}Be particles could not be measured with the present experimental

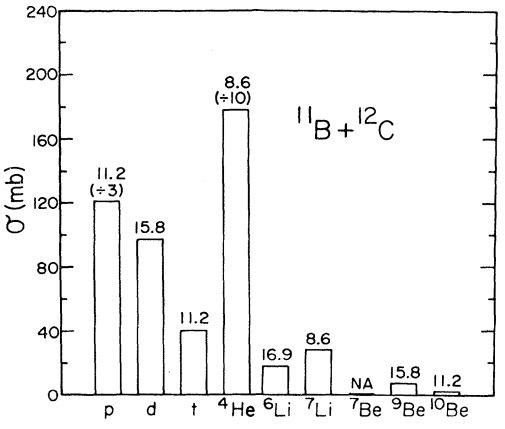

FIG. 11. Angle-integrated cross sections for the outgoing light particles produced in the $^{11}B+^{12}C$ reaction at 54 MeV.

TABLE I. Possible breakup channels for the ^{10}B and ^{11}B projectiles.

	Primary breakup
^{10}B	$p+^9Be$
	$d+^8Be$
	$t+^7Be$
	$^3He+^7Li$
	$^4He+^6Li$
^{11}B	$p+^{10}B$
	$d+^9Be$
	$t+^8Be$
	$^4H+^7Be$
	$^4He+^7Li$
	$^5He+^6Li$

setup and, therefore, have not been included in the present analysis, there is again no double counting problem. The same argument can be applied to the triton exit channel for the ^{11}B projectile. All other breakup channels, with the exception of $^{10}B \rightarrow t + ^{7}Be$ and $^{11}B \rightarrow d + ^{9}Be$, contain only one particle which is included in our analysis of the total breakup cross section. The two exceptions listed above would give rise to double counting if the system is left in a three-body final state. Since we have no reliable means for separating the two- and three-body contributions for these exit channels, we have simply included both the heavy and light particle yields in our evaluation of the total breakup cross section. While this allows the possiblity of double counting, the heavy particles involved are so weak ($\sigma < 7$ mb) that little change would occur in our estimate of the total breakup cross section.

For reactions leading to a two-body final state, the possible breakup channels are again listed in Table I. If the light member of each breakup pair is captured (i.e., transferred to the target nucleus), each breakup event is counted by the detection of the heavier fragment. If the heavy member of a particular breakup pair is captured, the event will be identified by the detection of the light fragment member for all exit channels except for the proton and alpha. Again we cannot determine the breakup cross section for these channels owing to our inability to distinguish between breakup and evaporation events. Therefore, while we may be slightly overestimating the total breakup cross section for three-body events as discussed in the preceding paragraph, we are underestimating the total breakup cross section when the system is left in a two-body final state accompanied by the emission of either protons or alpha particles.

Summing the d, t, and heavy-particle strengths for each of the two entrance channels, we find, as shown in Table II, that the $^{10}B+^{13}C$ breakup cross section is 290 mb while that for the $^{11}B+^{12}C$ system is 193 mb. If these cross sections are added to the experimentally measured fusion cross sections for each entrance channel,[1,2] then 82% of the $^{10}B+^{13}C$ and 92% of the $^{11}B+^{12}C$ total reaction cross sections, extracted from optical fits to the elastic scattering data,[2] are accounted for for these entrance channels. The remaining "missing" cross section may partially be due to the problem discussed above concerning the p and α particle exit channels, may simply reflect the uncertainty associated with measuring the absolute magnitudes of the fusion, breakup, and total reaction cross sections or may be due, at least partially, to reaction mechanisms not yet investigated (e.g., inelastic scattering). To help resolve this question, future experiments will involve the measurements of the inelastic scattering cross sections.

TABLE II. Cross sections for various reaction mechanisms for the $^{10}B+^{13}C$ and $^{11}B+^{12}C$ entrance channels at a bombarding energy of 54 MeV.

Reaction mechanism	System $^{10}B+^{13}C$ (mb)	$^{11}B+^{12}C$ (mb)
Breakup	290	193
Fusion[a]	890	1064
Sum[b]	1180	1257
Total reaction[c]	1434	1360

[a]See Refs. 1 and 2.

[b]Sum of experimentally measured breakup and fusion cross sections.

[c]Total reaction cross section obtained from an optical model fit to elastic scattering data. For additional details see Ref. 2.

Finally, if we again look at the energy distributions of the various outgoing particles, one finds for many of the exit channels that the data are qualitatively in better agreement with the Serber model calculations when a three-body reaction process has been assumed. A few cases exist where both particles which arise from the same breakup event can be observed. For these exit channels an upper limit can be placed on the three-body cross section. The dissociation of ^{11}B into a deuteron and a ^{9}Be nucleus is one such example. As can be seen in Fig. 11, the integrated ^{9}Be strength and, consequently, the maximum three-body cross section for this exit channel, is 7 mb. The remaining strength in this channel, $\sim$90 mb (the difference in the d and ^{9}Be integrated cross sections), could be produced by a number of different reaction processes. First, there is the possibility that the number of deuterons arising from compound nuclear evaporation has been underestimated. We believe that this is not the case, however, based upon the extensive nature and strong systematics observed in the earlier study of deuteron emission from compound nuclei in this mass and energy region.[13] Another reaction mechanism which could account for the missing ^{9}Be strength involves the direct transfer of ^{9}Be from the projectile to the ^{12}C target. As can be seen in Fig. 1, however, the deuteron energy distribution provides little support for this two-body final state interpretation in that no discrete states are observed and the two-body calculation does a poor job of describing the deuteron energy spectrum. Finally, it is possible that during breakup the ^{9}Be nucleus is excited to one of its particle unstable states and decays before being detected. It might be noted that in p, d, and α particle inelastic scattering on ^{9}Be targets a particle unstable state at 2.43 MeV is strongly populated.[14] Integrated cross sections for the 2.43 MeV level in this study range from 44 to 110 mb depending upon the projectile and energy involved.

To investigate the effect that exciting the ^{9}Be nucleus to its 2.43 MeV level would have on the deuteron energy distribution, Serber model calculations which account for this process have been performed and are presented in Fig. 13. As can be seen, the yield from such a process, if present, could not be readily distinguished from three-body events. If this process is indeed important, then earlier breakup studies[9,10] which have excluded the yield to the light-particle exit channels (p, d, t, and α) may have severely underestimated the magnitude of the total breakup cross section. To fully resolve this question, particle-particle coincidence studies appear to be necessary. Such measurements are currently being planned.

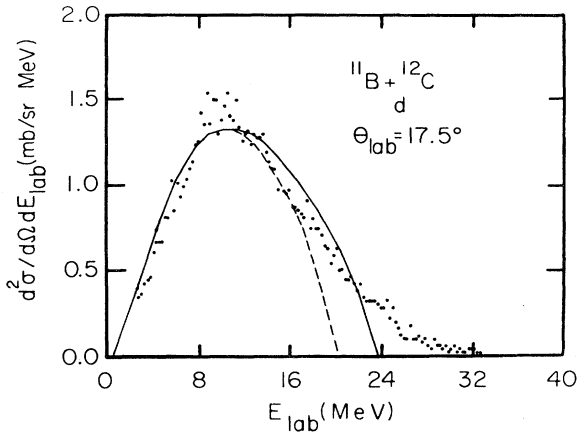

FIG. 13. The $^{11}B+^{12}C$ deuteron energy spectrum at $E_{lab}=54$ MeV and $\theta_{lab}=17.5°$. The solid curve represents a fragmentation model prediction based on a three-body final state with all outgoing nuclei in these ground states. The dashed curve represents a fragmentation model prediction based on a three-body final state in which the deuteron and target nucleus are in their ground state while the ^{9}Be nucleus has been excited to 2.43 MeV.

IV. SUMMARY

In conclusion, the spectra of particles lighter than the projectile exhibit strong continuum structures for both the $^{10}B+^{13}C$ and $^{11}B+^{12}C$ reactions. The energy centroids of these continuum structures correspond to approximately the beam velocity. The shapes of the energy spectra and angular distributions are explained reasonably well by a simple breakup model involving one free parameter (K, the overall normalization constant). These calculations take into account the internal momentum of the fragments based on their separation energy, assume that the final state consists of either two or three bodies, and use a local momentum approximation to account for the Coulomb distortions of the incoming and outgoing waves. Our results suggest a substantial breakup cross section, $\sim$200 mb for the $^{11}B+^{12}C$ entrance channel and $\sim$300 mb for the $^{10}B+^{13}C$ system, even at the relatively low bombarding energy of 54 MeV. When these cross sections are added to our previously measured fusion cross sections,[12] 82% of the $^{10}B+^{13}C$ and 92% of the $^{11}B+^{12}C$ total reaction cross section strengths are accounted for. Finally, the possibility has been discussed that there may be significant contributions from breakup processes which result in final states of four or more bodies.

ACKNOWLEDGMENTS

It is a pleasure to acknowledge the many productive discussions we have had during the course of this work with Dr. S. L. Tabor, Dr. L. C. Dennis, and Dr. K. W. Kemper from Florida State University. The assistance of Douglas Fields, Greg Wheatley, and Neville Newman in the collection and analysis of the data is also appreciated. This research was supported in part by the U. S. Department of Energy under Contract No. DE-AS05-80ER10714 and by the National Science Foundation.

[1]J. F. Mateja, A. D. Frawley, L. C. Dennis, K. Abdo, and K. W. Kemper, Phys. Rev. Lett. 47, 311 (1981).
[2]J. F. Mateja, A. D. Frawley, L. C. Dennis, K. Abdo, and K. W. Kemper, Phys. Rev. C 25, 2963 (1982).
[3]J. Gomez del Campo, R. G. Stokstad, J. A. Biggerstaff, R. A. Dayras, A. H. Snell, and P. H. Stetson, Phys. Rev. C 19, 2170 (1979).
[4]J. J. Kolata, R. M. Freeman, F. Haas, B. Heusch, and A. Gallmann, Phys. Rev. C 21, 579 (1980).
[5]R. Serber, Phys. Rev. 72, 1008 (1947).
[6]J. R. Wu, C. C. Chang, and H. D. Holmgren, Phys. Rev. Lett. 40, 1013 (1978).
[7]C. K. Gelbke, M. Bini, C. Olmer, D. L. Hendrie, J. L. Laville, J. Mahoney, M. C. Mermaz, D. K. Scott, and H. H. Wieman, Phys. Lett. 71B, 83 (1977).
[8]E. Takada, T. Shimoda, N. Takahashi, T. Yamaya, K. Nagatani, T. Udagawa, and T. Tamura, Phys. Rev. C 23, 772 (1981).
[9]S. L. Tabor, L. C. Dennis, K. W. Kemper, J. D. Fox, K. Abdo, G. Neuschaefer, D. G. Kovar, and H. Ernst, Phys. Rev. C 24, 960 (1981).
[10]S. L. Tabor, L. C. Dennis, and K. Abdo, Phys. Rev. C 24, 2552 (1981).
[11]N. Matsuoka, A. Shimizu, K. Hosono, T. Saito, M. Kondo, H. Sakaguchi, Y. Toba, A. Goto, F. Ohtani, and N. Nakanishi, Nucl. Phys. A311, 173 (1978).
[12]It should be emphasized here that with the present experimental arrangement we have no way of distinguishing between the three-body reaction process depicted in Fig. 7(b) and other types of reaction mechanisms which may leave the system in a three body final state, e.g., capture of one of the projectile fragments by the target followed by evaporation of this fragment from the target-fragment system.
[13]A. C. Xenoulis, A. E. Aravantinos, C. J. Lister, J. W. Olness, and R. L. Kozub, Phys. Lett. 106B, 461 (1981).
[14]R. G. Summers-Gill, Phys. Rev. 109, 1591 (1958).